

A comparative study of fractal models and U-statistic method to identify geochemical anomalies; case study of Avanj porphyry system, Central Iran

B. Shokouh Saljoughi*, A. Hezarkhani and E. Farahbakhsh

Mining and Metallurgical Engineering Department, Amirkabir University of Technology, (Tehran Polytechnic), Tehran, Iran

Received 13 August 2017; received in revised form 5 September 2017; accepted 20 September 2017

*Corresponding author: b.shokouh@aut.ac.ir (B. Shokouh Saljoughi).

Abstract

The most significant aspect of a geochemical exploration program is to define and separate the anomalous values from the background. In the past decades, geochemical anomalies have been identified by means of various methods. Most of the conventional statistical methods aiming at defining the geochemical concentration thresholds for separating anomalies from the background have limited the efficiency in the areas with complex geological settings. In this work, three methods including the Concentration-Area (C-A) and Spectrum-Area (S-A) fractal models, and the U-statistic method are applied to identify the geochemical anomalies in Avanj porphyry system due to a complex geological and tectonic setting. The results obtained show that the S-A and U-statistic methods present more acceptable outputs than the C-A method. The C-A model acts well to identify the geochemical anomalies within a region including a simple geochemical background; however, the model has limitations within a region including a complex geological setting, where each sub-area is characterized by different geochemical fields. The U-statistic method, by considering the location of sampling points, their spatial relation, and radius of influence for each point in the estimation of anomaly location, overcomes the limitations of the C-A model. The S-A model is a powerful tool to decompose mixed geochemical patterns into a geochemical anomaly map and a varied geochemical background map. The output of this method shows the analysis of geochemical data in the frequency domain, which can provide new exploratory information that may not be revealed in the spatial domain. Eventually, it can be pointed out that the accuracy of the S-A fractal model for determining the thresholds is higher than the other two methods mentioned.

Keywords: *C-A Fractal, S-A Multi-Fractal, Geochemical Anomaly, Anomaly Separation, U-Statistic, Avanj Porphyry System.*

1. Introduction

Geo-anomaly is a geologic body or geologic body combination that is different from its adjacent settings in composition, texture, structure, and genetic sequence [1-3]. A geochemical anomaly is a region where the concentration of a specific element is greater than a certain threshold value which is conventionally determined by statistical parameters such as mean, median, mode, and standard deviation [4-6]. It occurs either by common geological processes over long periods of time related to different geological events (e.g. tectonics, weathering, and erosion) or uncommon processes such as mineralization, human

activities, and element dispersion from an ore body [7-9]. Delineation and separation of geochemical anomalies from background is one of the most fundamental tasks in the fields of mineral exploration and mineral resource assessment because they have a profound influence on the analysis of geological evolution and mineralization process. Usually determination of the thresholds are the main key to geochemical data processing in order to separate anomalies from the geochemical background, and then either delineate the mineralized areas or distinguish the

anthropogenic and natural sources of materials [10, 11].

In the past 30 years, specialized methods and strategies have been developed for identifying the geochemical anomalies from the background. The properties on which one can differentiate distinctive populations of geochemical data may include the geochemical value frequency, spatial variability of geochemical values, geometrical characteristics of anomaly, and scaling properties of a geochemical anomaly [12-15]. The most effective way to distinguish the geochemical anomalies from the background is to adopt a comprehensive technique that combines the properties mentioned above. In general, methods for separating geochemical populations may be broadly classified into the non-structural and structural approaches. The non-structural methods consider only the frequency distribution of an element concentration, and ignore the spatial variability. In particular, information about the spatial correlation is not always available. In addition, these methods are only applicable to cases where the geochemical data follows a normal distribution. Nevertheless, the normal distribution does not provide the only possible model of geochemical distribution [6]. Furthermore, the gathered data has to be modified in non-structural methods, e.g. by rejection of outliers and normalization of data. Moreover, the conventional statistical methods that use histogram analysis or Q-Q plots assume normality or lognormality of the data, and do not consider the shape, extent, and magnitude of the anomalous areas [16]. For this sake, the structural approaches emerged.

Structural methods involve frequency distribution, spatial variability, and correlation, and they include various forms of spatial statistics and filtering. Within this, there is an increasing use of the fractal models and U-statistic method [17-19]. Cheng (1999b) has first presented the U-statistic method [20]. Indeed, this method is strong for separating the anomaly from the background [21], and it is based upon moving window techniques with an optimal variable window shape and size. The U-statistic values are calculated for each specific point using the surrounding points, which shows that there is a spatial relation between them [20, 22]. The main problem of this method is that it does not consider the geometry of the anomalous areas since the geometry of a geochemical anomaly may provide clues for anomaly interpretation. For example, linear anomalies may imply structural controls, and

arcuate anomalies may be associated with intrusive or deformed bodies. It has generally been accepted that the spatial and geometrical information of anomalies might be essential for anomaly separation. For this reason, the fractal/multi-fractal theory, as one of the subjects in non-linear mathematics, established by Mandelbrot (1983), considers the geometry property of geochemical landscape [23]. Since 1983, the fractal and multi-fractal models have extensively been applied to separate the anomalies from the background. These models include the number-size [24, 25] singularity indices [26], radial-density [27], concentration-distance [6], concentration-area [12], perimeter-area [28], concentration-volume [29], power spectrum-area fractal models [30, 31], and multi-fractal methods [32].

In this work, Avanj porphyry Cu-Mo system in Central Iran was chosen as the case of the study to compare the results from the Concentration-Area (C-A) and Spectrum-Area (S-A) models with U-statistic method, and to identify the geochemical anomalies associated with the mineralization. Furthermore, the effect of sampling density on the results is illustrated, and the edge effect in the S-A multi-fractal model was studied. This article is organized as follows. In the next section, the case study is investigated from the aspects of regional geology, structural geology, and geological setting. In Section 3, the geochemical dataset and statistical calculations are described. Section 4 gives a survey of the methods, their principles, advantages, and limitations. Section 5 describes the results, and Section 6 entitled "Discussion" compares the applied methods to demonstrate their efficiency. Finally, in Section 7, conclusions are presented.

2. Avanj Cu-Mo porphyry system

In terms of regional geology, Avanj porphyry system with an area of about 7 Km² is located in Central Iran on the Uromieh-Dokhtar magmatic belt. This belt is part of the Alpine-Himalayan orogenic belt. Tertiary volcanic rocks are the oldest geological unit in the study area. Intrusive bodies can also be observed at the edge of the district. Due to (i) the intensity, type, and zoning of the alterations, (ii) surface mineralization evidences, and (iii) contiguous geochemical anomaly of Cu and Mo at the center and Mn-Zn-Pb at the margins of the system, the study area can be considered as one of the highly potential reserves that typically involves Cu-Mo mineralization.

The main rock units in Avanj porphyry system, which is 90 Km far from the northeast of Isfahan and 5 Km distant from the East of Avanj village, consist of andesite, porphyry dacite, rhyodacite, quartz diorite, and diorite along with quartz-magnetite veins. Common alterations in a porphyry system including phyllic (quartz-sericite), argillic (quartz-clay minerals), and propylitic (chlorite-epidote) alterations, and also various iron oxide minerals (jarosite, hematite, and goethite) can be observed in the study area. The geological map of the study area is shown in Figure 1. According to this map, alterations from the center to the margins include phyllic or quartz-sericite (mainly in the northern and southern sections), quartz-magnetite stockworks (mainly in the southern section), argillic (quartz-kaolinite), and propylitic (epidote and chlorite on the margins). Hydroxides of iron (hematite, goethite, and jarosite) are observed in most places relating to phyllic and argillic alterations.

The porphyry rhyodacite units aged Miocene and they are observed in brown color on the ground. This unit contains argillic alteration, goethite oxides sporadically, and jarosite-silica veins. It also involves porphyry dacite and quartz-diorite rock units, and does not have appropriate hematite mineralization in relation to copper sulfide. The porphyry dacite unit aged Miocene is the most

important unit containing copper mineralization potential in the area. The unit includes quartz-sericite (phyllic) alteration, quartz-hematite stockworks, abundant iron oxide mineralization (mainly scattered and veinlets of hematite), and locally malachite mineralization. Dacitic rocks, located at the center of the southern and northern sections, include significant mineralization of hematite associated with copper sulfides. Quartz diorite intrusive bodies aged Miocene and include potassic alteration and quartz-magnetite veins. Diorite contains propylitic alteration intruded into semi-deep dacite-rhyodacite porphyry, and leads to the alteration of old rocks and creation of Cu-Mo mineralization in different parts of the phyllic alteration system. This unit can be seen in the central parts of the south porphyry alteration system. The quartz-diorite porphyry unit in the western part of the south porphyry system includes propylitic alteration.

Faults play an important role in the structure of tectonics, positioning of the igneous rocks, alteration and mineralization in the study area. Avanj porphyry system is tectonically located at the intersection of the Uromieh-Dokhtar magmatic belt and the furthest part of the Daroneh fault striking NE-SW. In general, the injection of intrusive bodies and fault mechanism play an important role in structuring the eastern part of the mentioned fault.

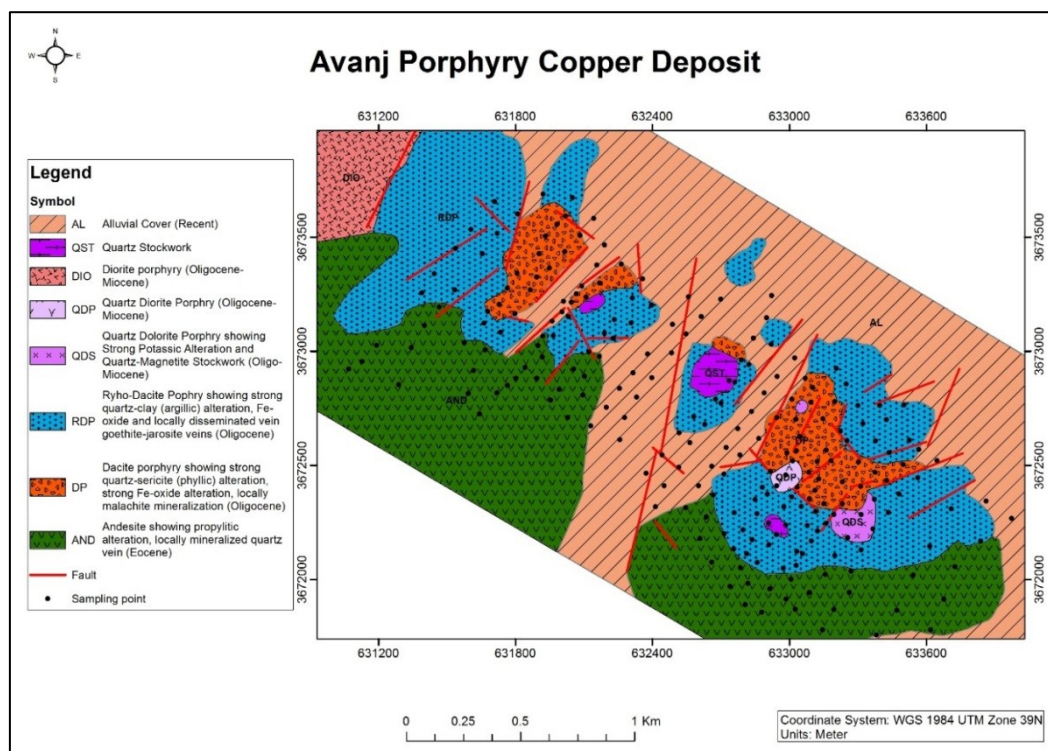


Figure 1. Geological map and lithogeochemical sampling locations of Avanj porphyry system.

3. Geochemical dataset

Geochemical surveys are an important part of geoscience investigations in both mineral exploration and environmental monitoring. A total number of 251 rock samples were collected in the study area using a semi-regular network and chip-sampling method so that the sampling density in volcanic units with high potential of mineralization like dacitic rocks is higher than the other units. These samples were analyzed by the ICP-MS method for 44 elements at Zarazma

laboratory, Tehran. Since Avanj deposit is known as a porphyry Cu-Mo system based on the mineralogical, geological, and geochemical results, these two elements were selected for the current study. The statistical parameters of Cu and Mo are presented in Table 1. The mean values for Cu and Mo are, respectively, 84.688 ppm and 4.9961 ppm, and their distributions are not normal. Histograms of the Cu and Mo concentration are shown in Figure 2.

Table 1. Statistical parameters of Cu and Mo elements in rock samples.

	N*	DL**	Accuracy	Min.	Max.	Mean	StD***	Variance	Skewness	Kurtosis
Cu	240	1 ppm	1	1	1040	84.688	147.2839	21692.542	3.738	16.457
Mo	251	0.5 ppm	0.01	0.83	89.60	4.9961	11.45388	131.191	4.671	25.902

* Some samples are removed from the study due to low value under the detection limit.

** Detection limit.

*** Standard deviation.

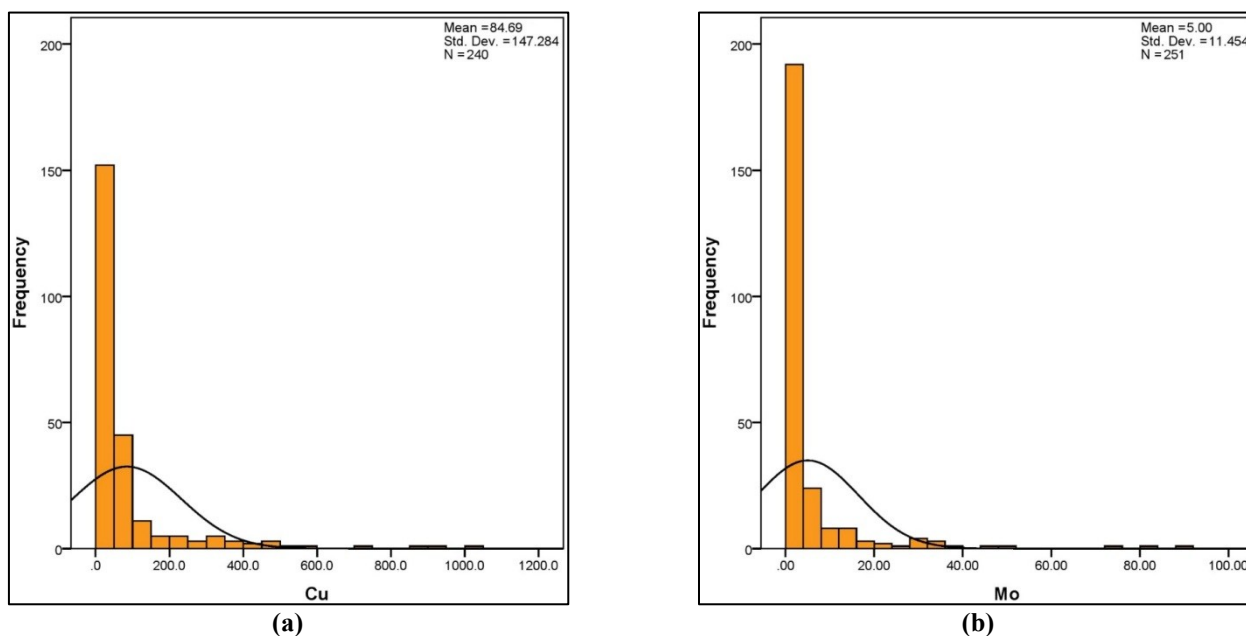


Figure 2. Histograms of a) copper and b) molybdenum concentration values in Avanj porphyry system.

4. Threshold determination methods

4.1. U-statistic method

The U-statistic method is one of the most important univariate structural methods that consider the spatial situation of samples. This method is based on moving the average technique with variable window radius [33, 34]. Assume a circle with the center of α_i (i-th sample position in the study area), a neighborhood radius of r ($0 \leq r \leq r_{max}$), and x_i as the desired quantity in this coordinate. Similar to all methods of calculating the weighted average, the closer points are more weighted than the further ones. After calculating the weight of each sample, the

dispersion of samples can be calculated as presented in Eq. (1) [20].

$$S_i(r) = \sqrt{\sum_{j=1}^n w_j^2(r)} \quad (1)$$

where $W_j(r)$ refers to the weights that are a function of the search radius. As a result, the U value in the i-th point with an effect of $S_i(r)$ on $\bar{x}_i(r)$ and standardization is defined as Eq. (2) [20].

$$U_i(r) = \frac{(\bar{x}_i(r) - \mu)}{\sigma} \quad (2)$$

in which μ is the mean and σ is the standard deviation of all the data. $U_i(r)$ is a function of r , and different values for U_i are obtained by changing r . For each r , the specific number of surrounding samples are considered for determining the U value of the unknown point. As a result, various U values are obtained for unknown points, and thus the optimal value for r is obtained for the maximum absolute value of U that causes the most separation between the two populations of anomaly and background [20, 33].

$$|U_i^*| = \max_{0 \leq r \leq r_{\max}} |U_i(r)| \quad (3)$$

Eq. (3) means that at each sampling point, the U values should be calculated from $r = 0$ to $r = r_{\max}$ and then from the U values that were obtained; the maximum value is devoted to the target point [20]. Although this method considers the frequency distributions and also spatial variability and correlation, it does not consider the geometrical characteristics of the anomaly and the scaling properties of a geochemical anomaly, which is one of the shortcomings of this approach.

4.2. Concentration-Area (C-A) fractal model

The C-A model [12, 13] is one of the most widely used fractal models. The C-A model, originally developed by Cheng et al. (1994), represents the first important step in the fractal/multi-fractal modeling of geochemical data, and has been “a fundamental technique for modeling geochemical anomalies” [35, 36]. It can be expressed as Eq. (4).

$$A(\geq c) \propto c^{-\alpha} \quad (4)$$

In this model, the measure $A(\geq c)$ is the area enclosed by contours with values greater than or equal to c on a geochemical contour map. It can also be estimated using the box-counting techniques, which involves counting the number of pixels with averaged concentration values greater than or equal to c on interpolated geochemical images.

The exponent α may have different values for different ranges of c . If the geochemical data is composed of multiple populations (for example, a mineralization-related anomalous population and a background population), the distribution of the points on a $\log A(\geq c)$ - $\log(c)$ plot fits more than one line segment. Each line segment is presumed to represent a different population characterized by a different value of the exponent α . The right-most breakpoint joining the line segments is generally taken as the threshold for separating the

anomaly from the background [37, 38].

This method has the following advantages: (i) it is based upon a very simple empirical set of equations; (ii) the advantages of this method are essentially its simplicity and easy computational implementation [39-41] as well as the possibility to compute a numerical value of concentrations, i.e. the anomalous threshold, which is the most useful criterion for cross-examination of information with numerical data from different sources; (iii) unlike most conventional methods, the C-A method generates classes (zones) of pixel values on the basis of not only the pixel-value frequency distribution but also takes into account the spatial and geometrical properties of the real-world features on the ground; (iv) in the C-A procedure, the original element concentration data can be treated directly [42], and therefore, it is unnecessary to process the data with pretreatment of any smoothing procedure, thus enhancing recognition of a geochemical anomaly from the background. The approach is also applied for image classification, anomaly separation, and assigning color palettes for displaying remotely-sensed images.

The disadvantage of this method is that although the C-A model is useful to identify the geochemical anomalies within a region including a simple geological background, it has limitations within a region linked with a complex geological setting, where each sub-area is characterized by different geochemical fields [43]. When the study area is regarded as a whole mineral district regardless of different geological background and different geochemical field in a complex region, the C-A model could not identify the weak anomalies well. One can firstly divide the whole study area into sub-areas in terms of geotectonic background and geochemical field, and then use the C-A model in each sub-area. Even in this case, the weak local geochemical anomalies are not identified well [43].

4.3. Spectrum-Area (S-A) model

Fourier/inverse Fourier transformation has been generally used in time series analysis and signal processing [30, 31, 44]. Spectral energy density functions illustrate the power spectrum distribution in the frequency domain. Cheng et al. (2000) have developed the idea of the C-A model into the frequency domain, and have extended the S-A model to characterize the spectral energy density-area relationship [45]. The advantage of dealing with fields in the frequency domain is that some complex convolution operations in the

spatial domain for correlation analysis, filtering, and transformation can be simplified significantly [46, 47]. The S-A model is one of the most sophisticated methods in which the frequencies and spatial distributions are used. It is given as Eq. (5).

$$A(\geq S) \propto S^{-2d/\beta} \quad (5)$$

where S denotes the spectral energy density as a function of the wave number vector, $A(\geq S)$ denotes area in the unit of wave number with a threshold above S, β is an anisotropic scaling exponent, d is a parameter representing the degree of overall concentration, and \propto denotes proportionality [48-51].

The implementation of the S-A model can be achieved in three steps:

- Generating a raster map through interpolating the raw data using an interpolation method [15];
- Converting the raster map into the frequency domain using the Fourier transformation. A dataset consisting of the power spectrum density (S) and the area with power spectrum density greater than or equal to S is obtained and then plotted in a log-log graph. N ($N \geq 2$) straight lines can be fitted using the LS method. N filters are defined with N-1 cut-off values from N ranges of power energy spectrum (S) that possess distinct scaling properties of the S-A relation. The small cut-off value generally defines the anomaly filter, and the large cut-off value defines the background filter.
- The inverse Fourier transform functions are applied to convert the frequency components back to the spatial domain [52].

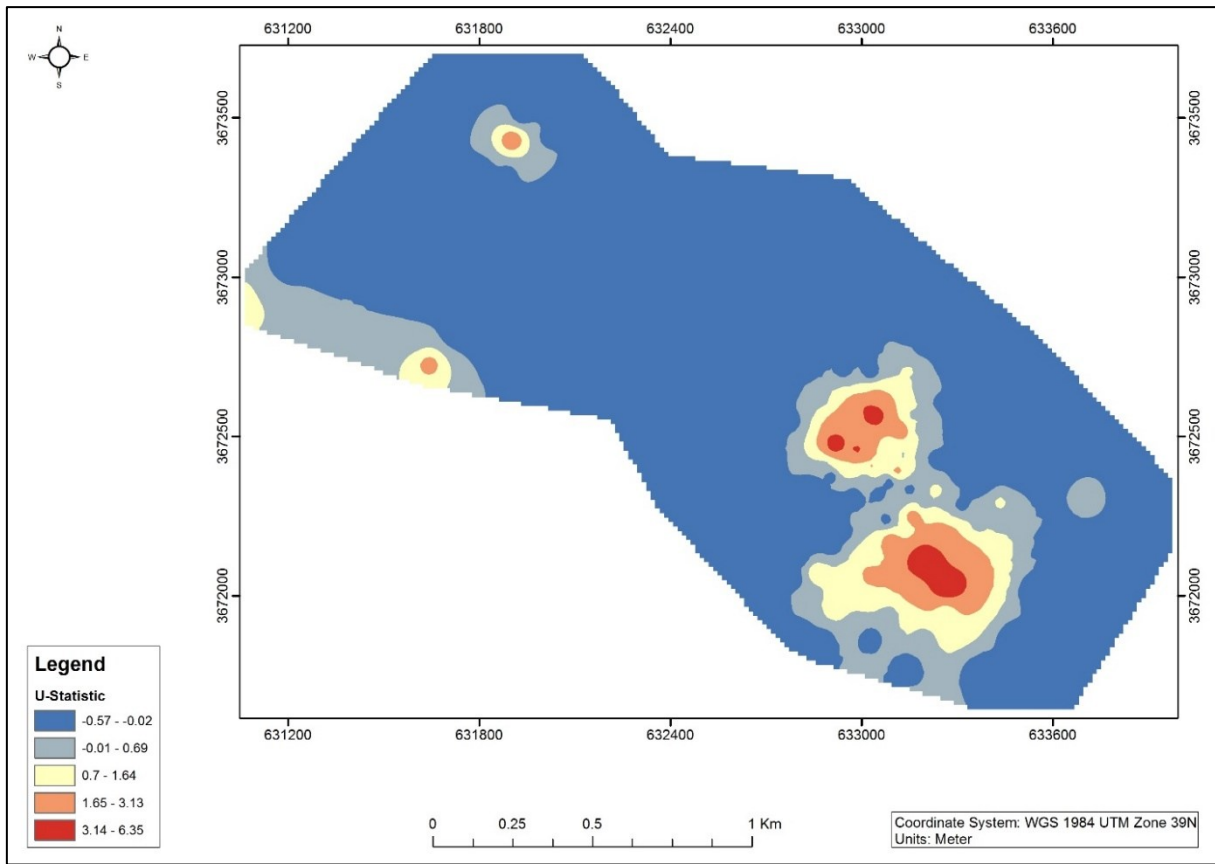
The main disadvantage of this method is that the resulting S-A model is influenced inevitably and sometimes severely by abrupt edge truncation [53-54]. The edge effects due to the irregular shape of the study area results in high values occurring at the edge of the study area. The edge effects in an irregular-shaped study area should be further investigated. Traditional solutions to reduce edge effects are too smooth for the boundary of the image prior to applying the Fourier transformation [45]. Zero-padding is one of the most frequently used smoothing methods [51]. This simple method can reduce the edge effect to some degree but it is inefficient in some applications when the image remains distorted. Moreover, due to the complexity of geoscience data involving irregular shapes and holes with missing data, zero-padding generally does not

give satisfactory results. Decay functions are suggested to handle edge effects in the geoscience image analysis [53]. A further study can focus on how to reduce the edge effects for the S-A model because the decay functions also cannot effectively reduce the edge effects for an irregular study area illustrated by Zuo et al. (2013) [43]. Recently, Afzal et al. (2017) have used the fractal-wavelet analysis to transform data from the spatial domain to the frequency domain [55].

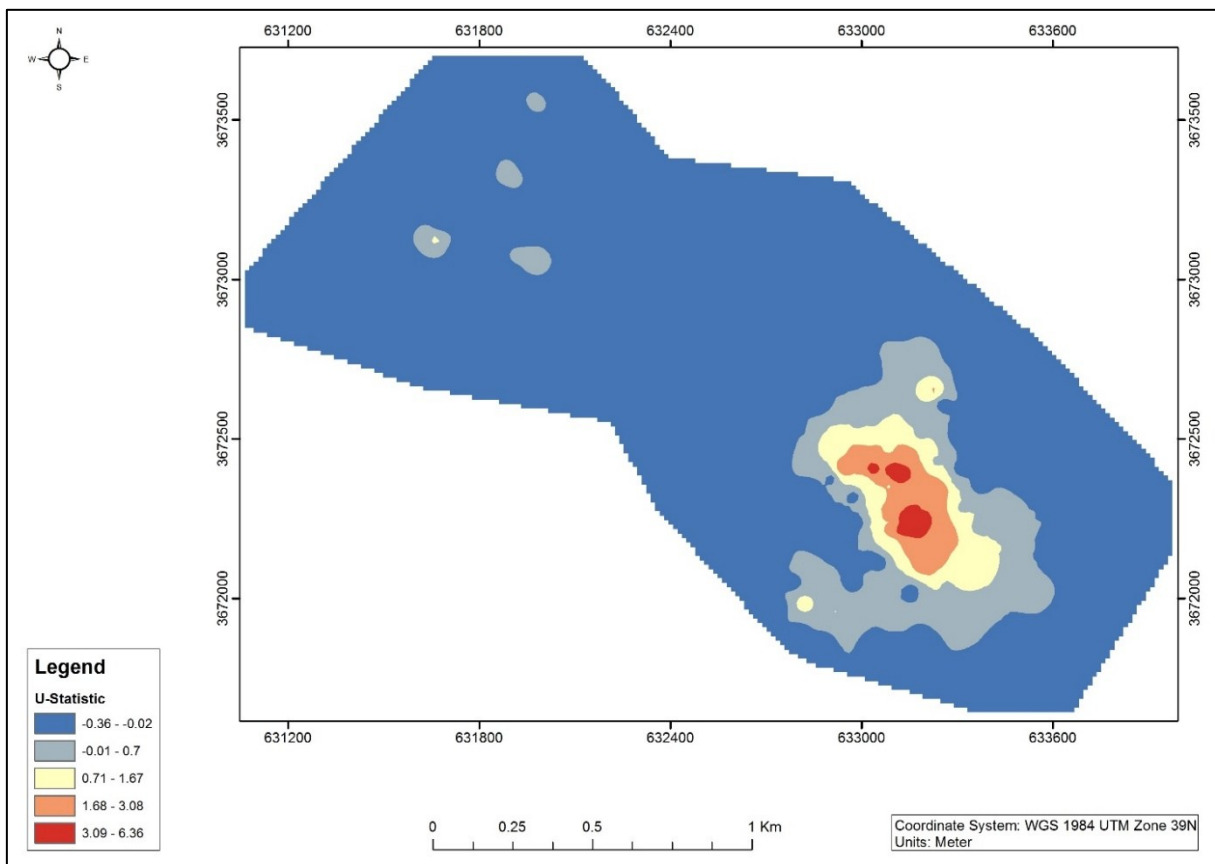
5. Results

5.1. U-statistic method

In this study, the copper and molybdenum anomalies were separated from the background by applying the U-statistic method. In this method, the radius value mostly depends on variables such as the average distance between the samples and the extent of the area in which the study is being carried out. Therefore, in this study, according to these variables, a range of different radii were considered for calculation of the U values. The average distance between the samples is calculated using a MATLAB code. The code calculates the distance of each sample point from the others, and then it considers the first eight minimum distance values for each point. The average of these values is calculated for each point, and finally, the mean of averaged values is considered as the average distance between the samples in the study area. The calculated value in the study area equals roughly 140 m. The radius range, which is considered for calculating the U values, includes 50 different radii, and it starts from the average distance quarter with the same increment that is equal to that. Following the calculation of U values, an interpolated raster map should be generated. The IDW interpolation method was used in this study for interpolating the U values, and the cell size was considered to be 14 m. This cell size is actually one-tenth of the average distance, which is considered as an appropriate cell size for the interpolation process according to the interpolated values for some check points. Based on the Jenks clustering method, the anomaly maps for Cu and Mo were plotted, as shown, respectively, in Figs. 3a and 3b. According to the outputs of this method, strong anomalies of both Cu and Mo could be observed at the southeastern section of the study area and a weak small anomaly at the northwestern section. The point to be considered is that the anomalies are mostly located over the dacite porphyry lithological unit, which shows a strong phyllic alteration.



(a)



(b)

Figure 3. a) Cu and b) Mo anomaly maps using U-statistic method.

5.2. Concentration-Area (C-A) fractal model

The C-A fractal model is one of the common and simple fractal methods that is based on the grade variations, the area it covers, and the higher grades to deal with the estimation of the cut-off grade and separation of the anomaly from the background. This method has been used to analyze various types of geochemical data including stream sediment samples [5, 13], rock samples [12], and humus [40]. In this study, the C-A method, proposed by Cheng et al. (1994), was used for separating the anomalies from the background. The steps of separating anomaly by this method can be summarized as follows: First, the geochemical data is interpolated by considering an appropriate interpolation method and an appropriate cell size. Then the area that is covered by a specific concentration value is determined. Next, the concentration values are sorted in ascending order, and the cumulative area for each value is calculated. The log-log plot of concentration versus area is generated and the straight trend lines are fitted on points. Finally, the threshold values occurring on the break points are extracted and the anomaly map is provided based on them.

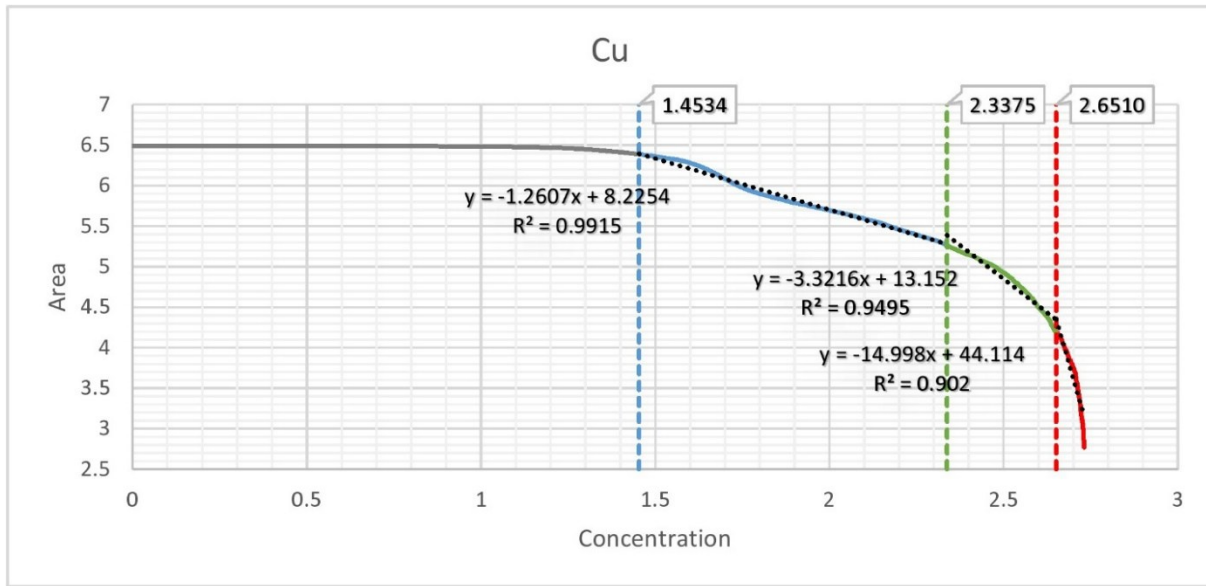
In this study, the C-A fractal model is implemented using MATLAB, and the maps are provided by ArcGIS. Figure 4 shows the log-log plots of concentration versus area for the elements Cu and Mo. Straight lines are fitted by means of the Least Squares (LS) method. In general, the fractal dimensions increase from lower to higher concentration populations. Low fractal dimensions are typical of the assumed background population distributions and high fractal dimensions typical of mineralization effects in the

study area. In Figures 4a and 4b, respectively, the values less than 1.4534 and -0.0167 (blue line) represent the depletion region and the values greater than 2.6510 and 1.5166 (red line) show the enrichment area but by various intensities. Three break points were considered for both plots, which were the threshold values for separating different populations of concentration values including anomaly and background. In Table 2, the break point values of log-log plots and their equivalent concentration value before taking logarithm for the two elements are given. According to this table, the threshold values that can be considered for separating the anomalies of Cu and Mo are, respectively, equal to 447.7346 and 32.8552.

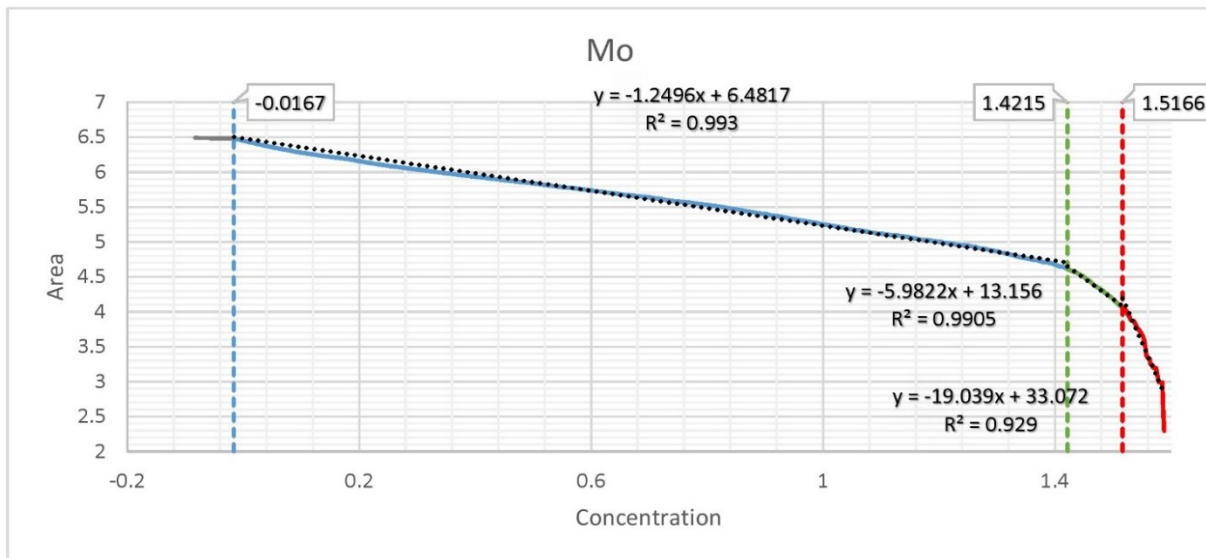
The geochemical maps of copper and molybdenum, which are classified by applying the C-A fractal model, are shown in Figure 5. According to these maps, the red class indicates the anomalous area and the blue class represents the depletion regions. The major anomaly areas, according to Figure 5, are located in the southeastern section of the study area. The Cu and Mo anomalies are well well-conformed and are spatially coincident with the tectonic activities and typically the faults. The classes that are representatives of different geochemical populations are more dispersed in comparison with the U-statistic outputs, and show a less coherent structure. The intense anomaly areas located at the southeastern section are placed over the dacite porphyry lithological unit, which shows a strong phyllic alteration. The anomaly section that was shown at the northwest of the study area by the U-statistic method has been somewhat diminished in this method.

Table 2. Break point values of C-A log-log plot and their equivalent concentration values before taking logarithm.

Element	Break point 1	Break point 2	Break point 3
Cu	1.4534	2.3375	2.6510
	28.4070	217.5155	447.7346
Mo	-0.0167	1.4215	1.5166
	0.9622	26.3942	32.8552

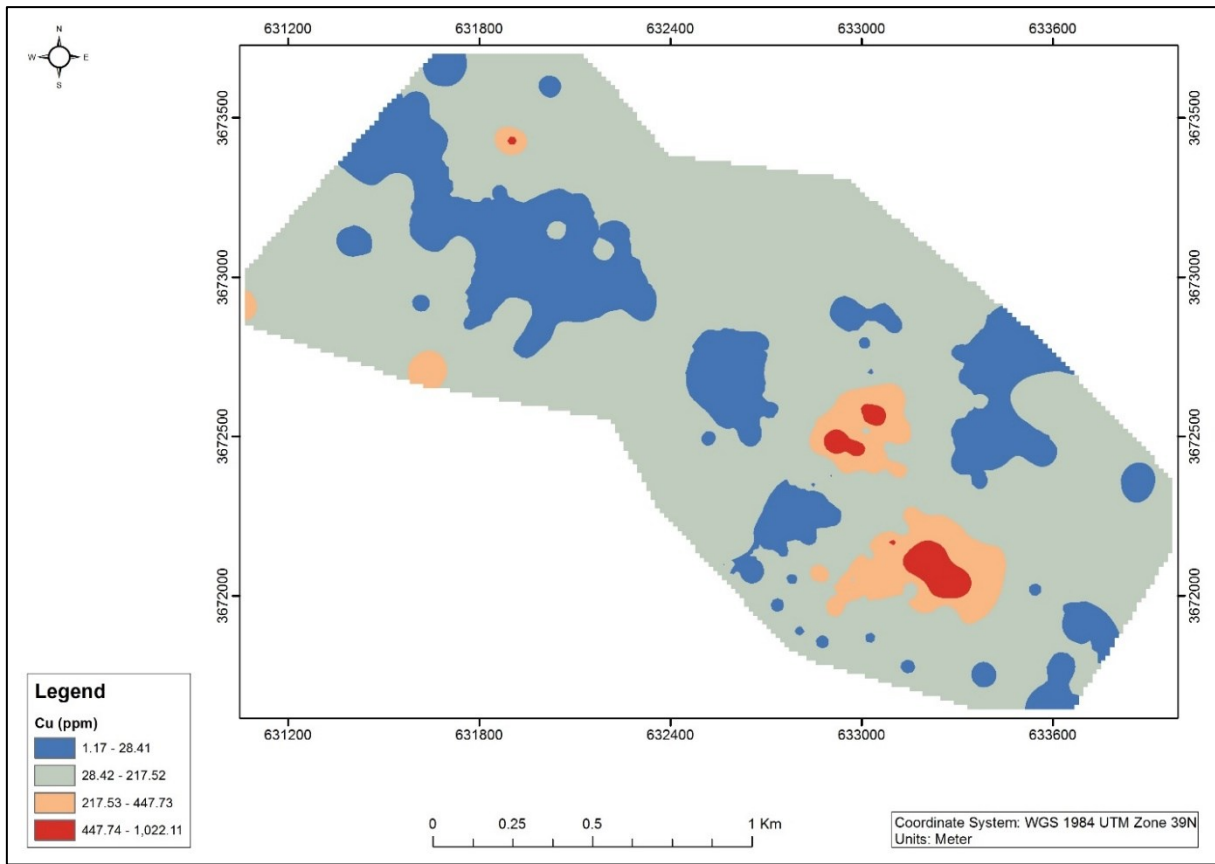


(a)

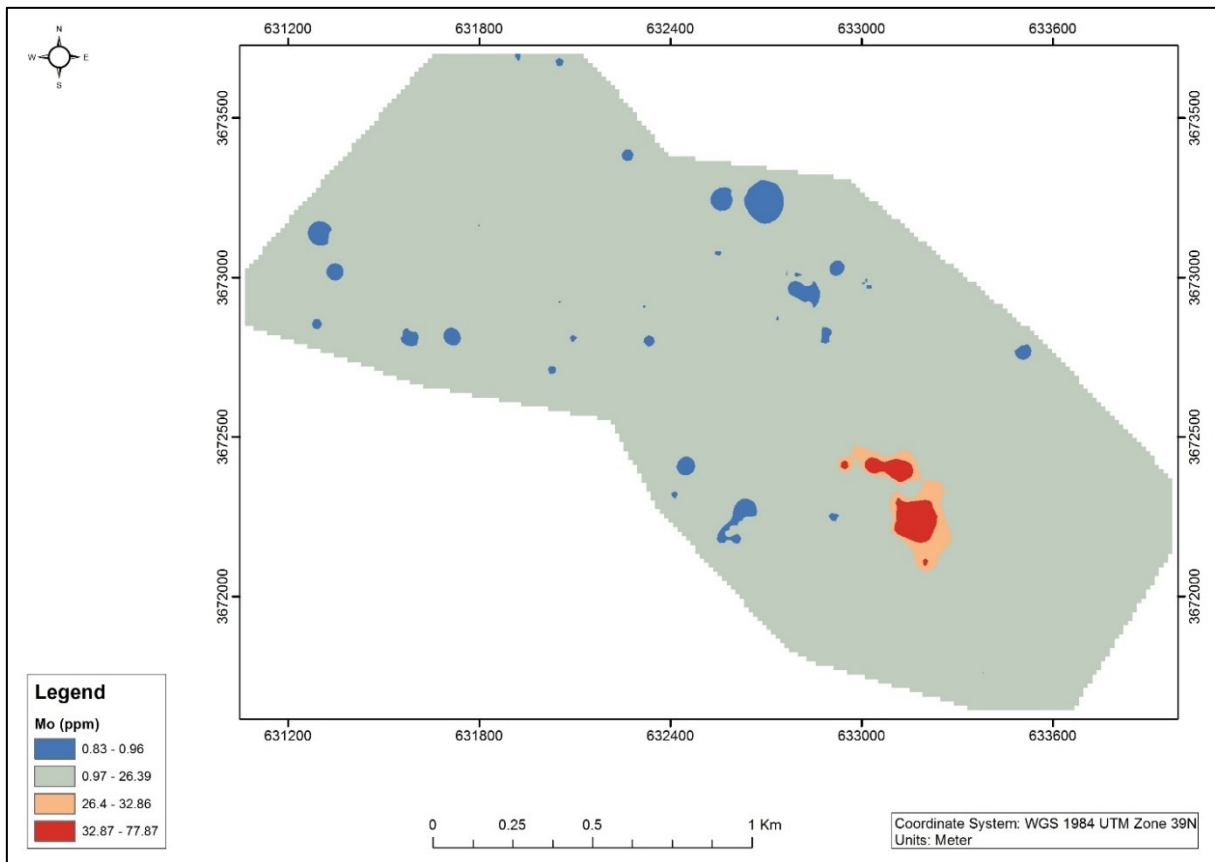


(b)

Figure 4. a) Log-log plot of concentration versus area for Cu b) log-log plot of concentration versus area for Mo.



(a)



(b)

Figure 5. a) Cu and b) Mo anomalies obtained from C-A fractal model.

5.3. Spectrum-Area (S-A) fractal model

The spatial distribution of Cu and Mo obtained using the inverse distance weighted (IDW) method through ArcGIS shows a mixed and complicated pattern. The S-A technique is used to decompose this mixed pattern. Firstly, the Cu and Mo maps are taken into the frequency domain by means of the two dimensional (2D) Fourier transformation.

Two components, the power spectrum density and phases, are obtained. The spectrum energy density (S) and the area (A) enclosed by values greater than or equal to the threshold for copper and molybdenum are plotted on a log-log scale (Figure 6). The S-A method ensures that the power spectrum value S and the area A follow power law relationships, as shown by the fitted straight-line segments on the log-log axes. Different straight-line segments with different slopes represent different self-similarities, which usually correspond to different patterns in the spatial domain. For example, in this study, for the elements Cu and Mo, four straight lines can be fitted by means of the LS method. This gives four ranges of power energy spectrum S that maintain distinct scaling properties of the S-A relation. In the case of copper, the values $\text{Log } S_0 = 5.1423$, $\text{Log } S_1 = 6.3727$, and $\text{Log } S_2 = 6.8786$ define three thresholds. $S < S_2$ may represent the anomalies and the power spectrum, and $S > S_0$ usually corresponds to the background (Cheng and Grunsky, 1999). Similarly, in the case of molybdenum, the values $\text{Log } S_0 = 2.2763$, $\text{Log } S_1 = 3.9529$, and $\text{Log } S_2 = 4.2719$ define four straight lines.

Furthermore, three types of fractal filters can be constructed based on the log S-log A plot: low-pass, high-pass, and band-pass spectral energy density filters. The abscissa of the intersection points, as threshold S_0 or S_1 , is defined by two intersecting line segments on both sides of the two segments. The different slopes of these segments indicate that they meet different fractal characteristics. Usually three types of fractal filters are defined as follow, based on the log S-log A plot:

$$G_A(\omega) = \begin{cases} 1 & S(\omega) \leq S_0 \\ 0 & S(\omega) > S_0 \end{cases} \quad (6)$$

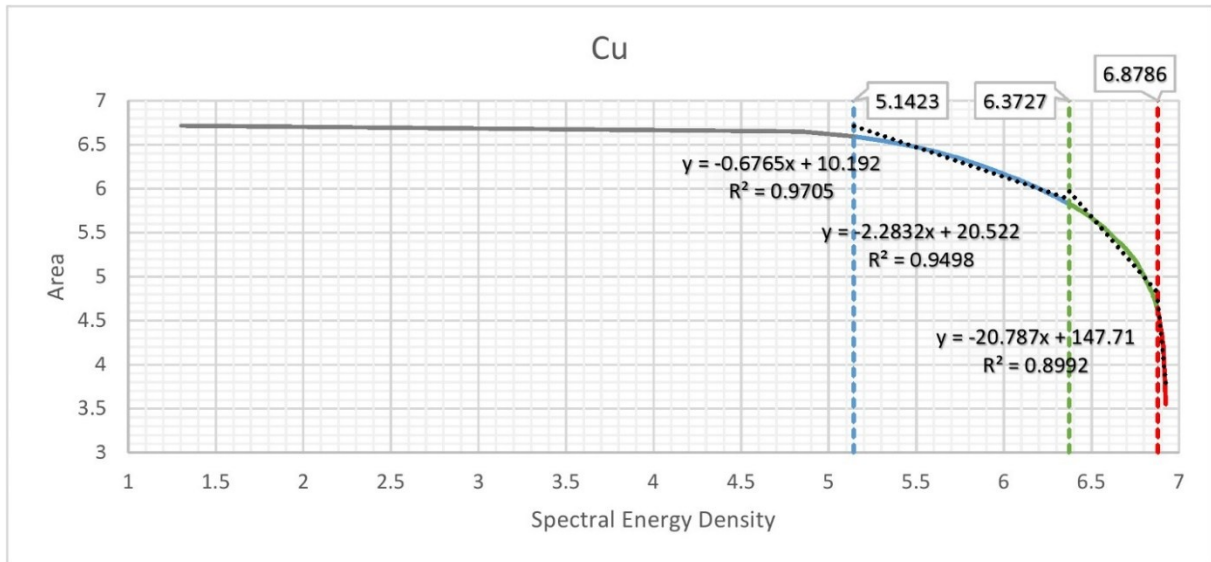
$$G_B(\omega) = \begin{cases} 1 & S(\omega) \geq S_2 \\ 0 & S(\omega) < S_2 \end{cases} \quad (7)$$

$$G_C(\omega) = \begin{cases} 1 & S_2 \leq S(\omega) \leq S_0 \\ 0 & \text{otherwise} \end{cases} \quad (8)$$

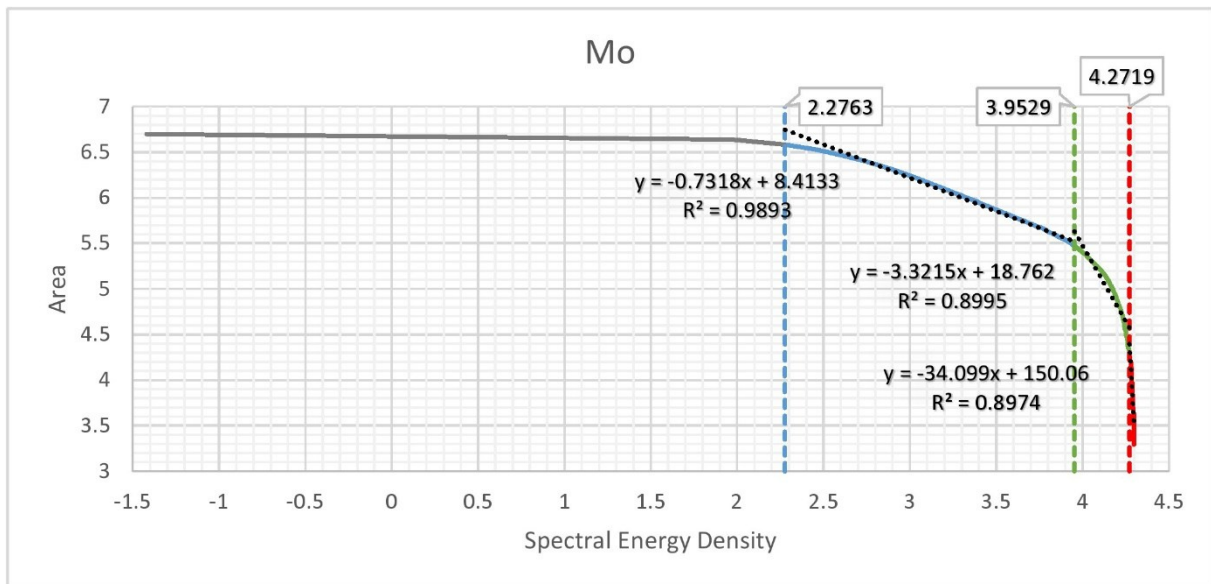
Investigations indicate that the spectral energy density is inversely related to the spectral frequency. It has also been proven that if $G_A(\omega)$ of the spectral energy density is less than $G_B(\omega)$, the wave number of $G_A(\omega)$ is larger than $G_B(\omega)$. In this sense, $G_A(\omega)$ corresponds to a high frequency and $G_B(\omega)$ to a low frequency. Therefore, $G_A(\omega)$ can be used as the high frequency energy spectral density filter and $G_B(\omega)$ is the low-frequency energy spectral density filter. Usually $G_A(\omega)$ can be considered as the anomaly filter and $G_B(\omega)$ can be considered as the background filter. $G_C(\omega)$ can be used to strain out energy spectra less than S_0 but greater than S_2 , retaining the spectral components within the interval (S_2, S_0) . In this way, $G_C(\omega)$ is a band-pass filter in a specific interval.

The resulting S-A model is influenced inevitably and sometimes severely by abrupt edge truncation [53, 54]. The edge effects due to the irregular shape of the study area result in high values occurring at the edge of the study area. The edge effects in this irregular-shaped study area should be removed. In Figure 7, the edge effects for Cu and Mo have been effectively addressed. There are various solutions to eliminate the edge effects [56-59]. In this work, we applied the zero-passing approach to reduce the edge effects. Zero-padding is one of the most frequently used smoothing methods. This simple method can reduce the edge effect to some degree.

After removing the edge effects and determining the thresholds, the high-frequency, low-frequency, and band pass filters are applied to the Fourier-transformed results, and then the inverse Fourier transform is applied to bring the data back to the spatial domain and the anomaly and background map was plotted. The Cu anomaly and background maps are obtained using the inverse Fourier transformation, which are shown in Figure 8. The promising areas of Cu mineralization are located in the areas with high background and anomaly values. The resulting anomaly and background maps for Cu and Mo are available, respectively, in Figures 8 and 9.

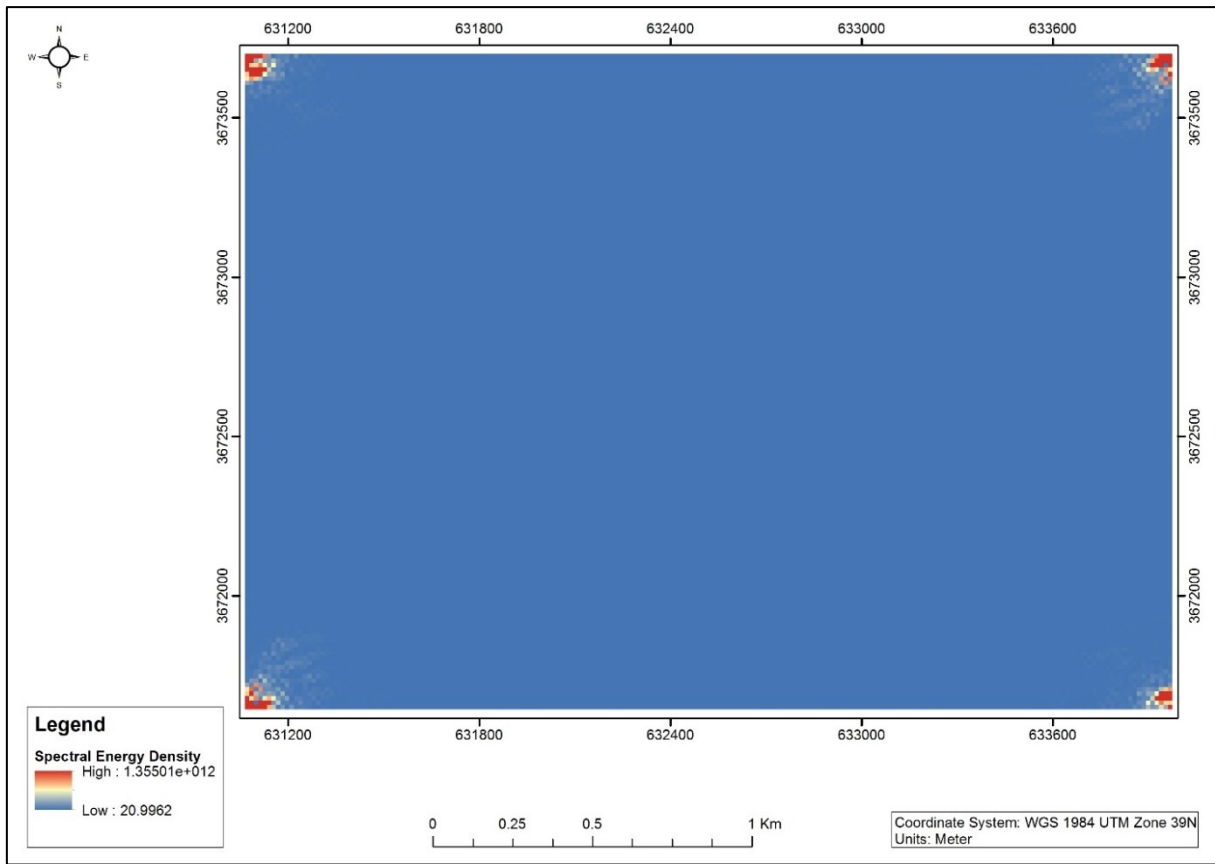


(a)

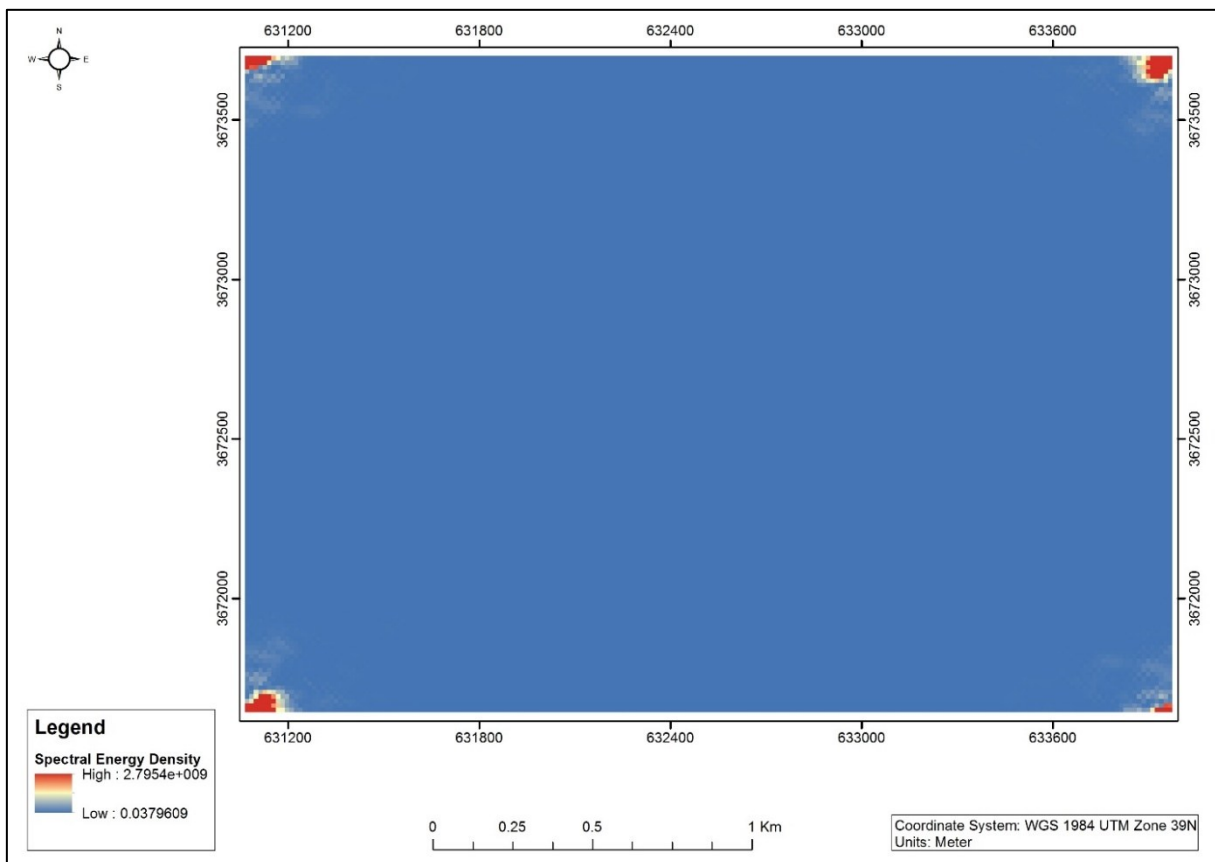


(b)

Figure 6. a) Log-log plot of power energy versus area of Cu and b) Mo.

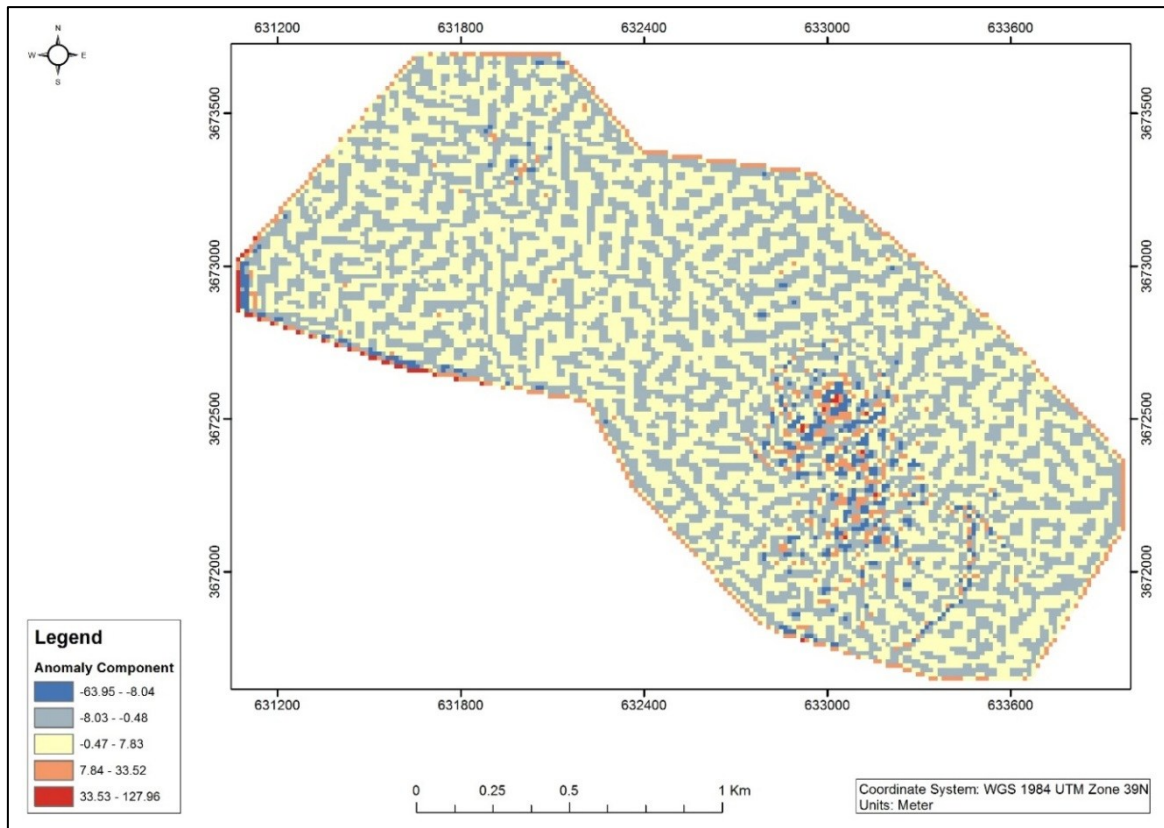


(a)

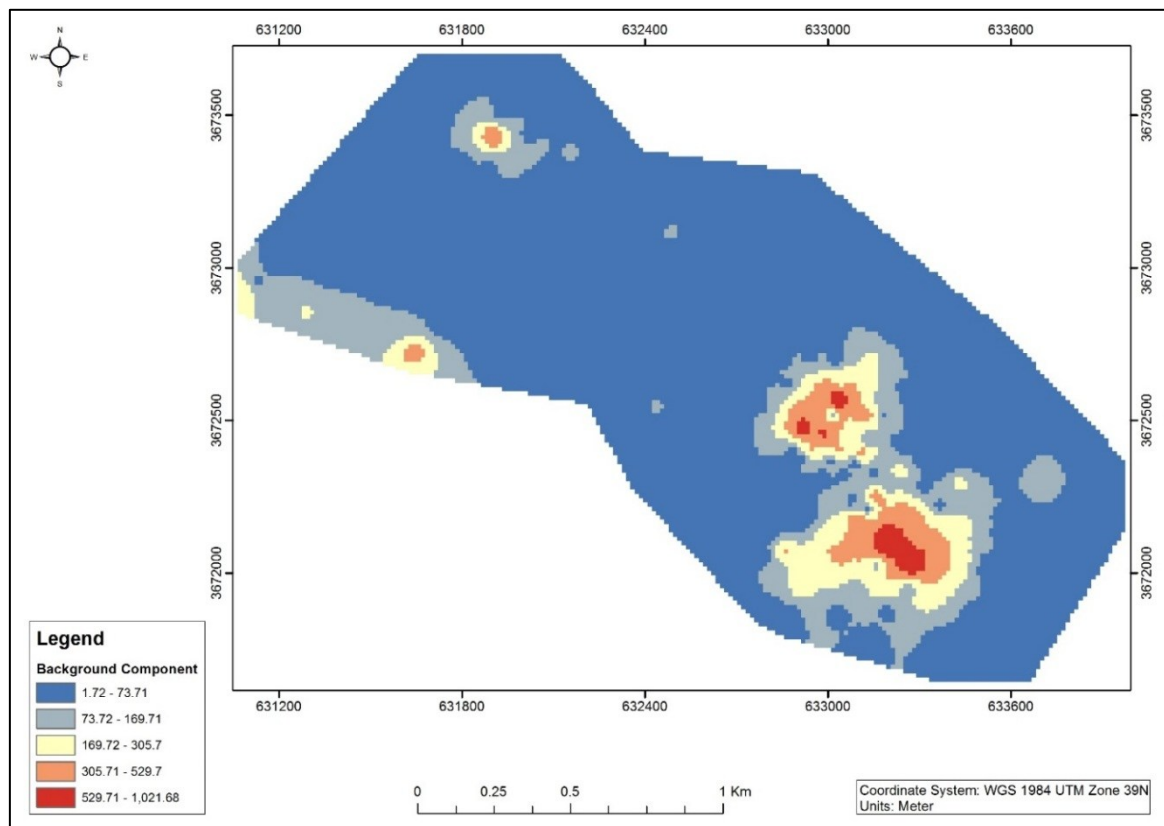


(b)

Figure 7. Edge effects for a) Cu and b) Mo.

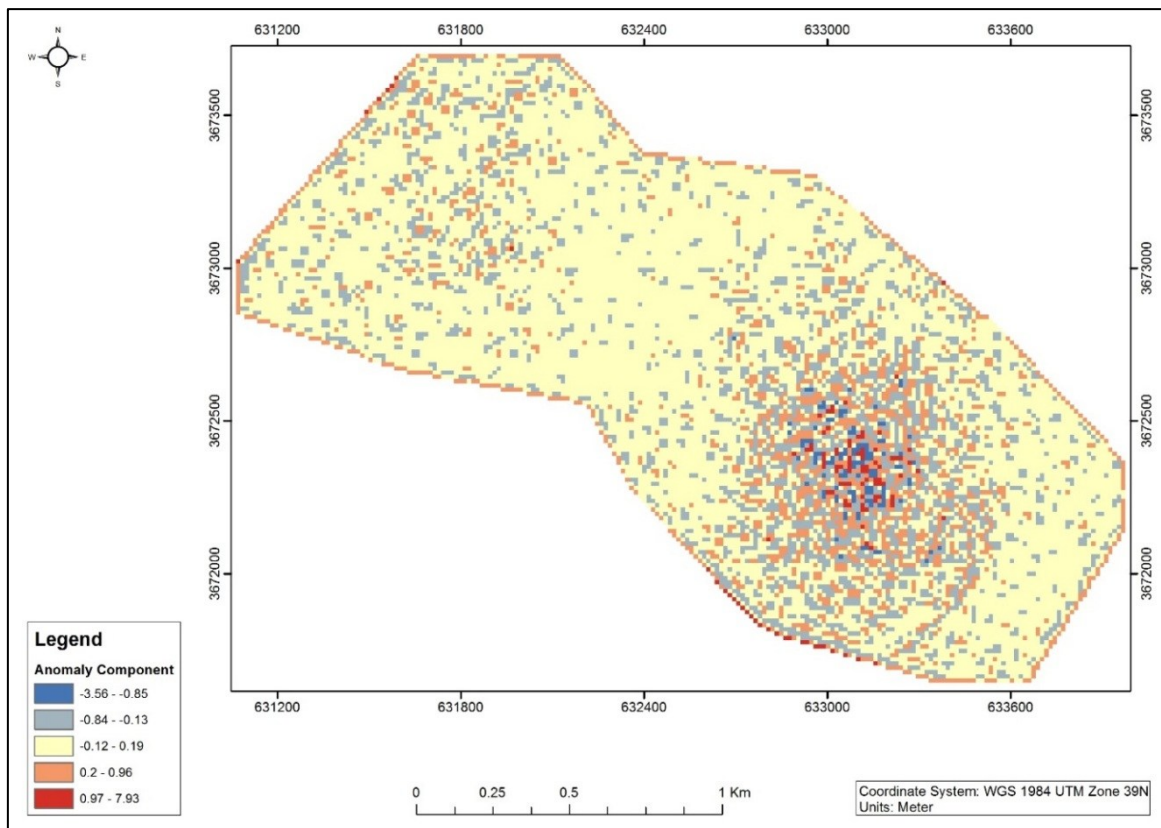


(a)

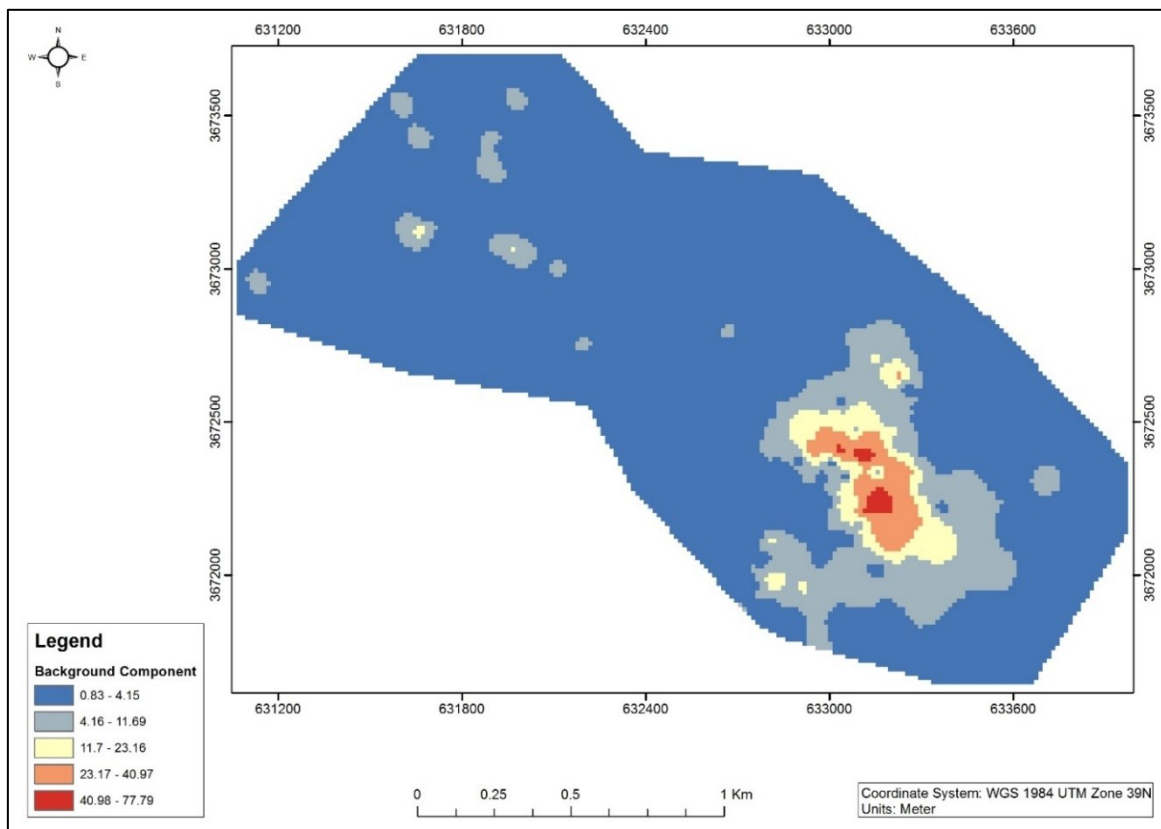


(b)

Figure 8. a) Anomaly and b) background maps showing promising areas of Cu mineralization using S-A fractal model.



(a)



(b)

Figure 9. a) Anomaly and b) background maps showing promising areas of Mo mineralization using S-A fractal model.

Considering the high values of the anomaly and background maps simultaneously for Cu and Mo, potential mineralization areas are mostly located at the southeastern section over the dacite porphyry lithological unit that shows a strong phyllic alteration associated with the hematite and malachite mineralization. The anomaly section seems more coherent in this method in comparison with the other two methods.

6. Discussion

In this study, three methods for anomaly separation including the C-A and S-A fractal models along with the U-statistic method were used. Each method has some advantages and limitations in different geological and structural settings. In what follows, we discuss the characteristics of the applied methods in comparison with each other. The C-A fractal model present four classes that can be considered from low to high values, respectively, as the background, possible anomaly, probable anomaly, and certain anomaly. Also the background class due to very low values of Cu and Mo can be classified as the depletion region. Dispersion of classes in the resulting map of the C-A method and low coherency of anomaly sections can be named as one of the limitations.

Output of the S-A fractal model mainly includes the two components anomaly and background. Sharp borders of the anomaly sections in both components can be considered as one of the characteristics of the S-A fractal model. The background component is somewhat similar to the output of the U-statistic method but the anomaly component is different, and the point that should be noted is that the anomaly sections with low sampling density are ignored in the anomaly component of the S-A fractal model. As an example, the anomaly section that is placed at the lower border of NW of the study area can be mentioned. Moreover, the conformity of the anomaly sections resulting from the S-A fractal model with potential lithological units is higher than the other two methods. For instance, the porphyry rhyodacite unit that includes a strong argillic alteration and iron-oxide does not show any considerable geochemical anomalies, whereas the dacitic rocks including strong phyllic alteration located at the center of the southern and northern sections show coherent and strong geochemical anomalies of copper-molybdenum according to the outputs of applying the S-A fractal model. Also the diorite unit containing the

propylitic alteration shows a weak geochemical anomaly in NW of the study area.

7. Conclusions

According to the complicated tectonic and intensive geological occurrences that have occurred in different periods of geological time, Avanj porphyry system has a complex geochemical surface expression. In such an intricate district, we need to apply several methods to separate the anomaly from the background. The most efficient way to distinguish the geochemical anomalies from the background is to adopt a comprehensive technique that combines the following properties: geochemical value frequency, spatial variability of geochemical values, geometrical characteristics of anomaly, and scaling properties of a geochemical anomaly. In this study, three methods including the Concentration-Area (C-A), Spectrum-Area (S-A), and U-statistic methods were applied to identify the geochemical anomalies in Avanj porphyry system (in Central Iran). The results of this study indicate the high ability of the fractal and U-statistic methods to separate the geochemical anomaly from the background. Based on the maps obtained, the U-statistic and S-A methods illustrate better results than the C-A method because the C-A model is useful to identify the geochemical anomalies within a region with a simple geochemical background but the model has limitations within a region linked with a complex geological setting where each sub-area is characterized by different geochemical fields and the whole region has a complex tectonic setting. When the study area is regarded as a whole mineral district regardless of different geological backgrounds and different geochemical fields in a complex region, the C-A model could not effectively identify the weak anomalies. The U-statistic method, by considering sampling point locations, radius of influence, and their spatial relation in the estimation of anomaly location, can overcome the disadvantage of the C-A model. It is a powerful tool to identify the geochemical anomalies within the regions characterized by a complex geological setting and a varied geochemical background. The S-A model is a powerful tool to decompose mixed geochemical patterns into a geochemical anomaly map and a varied geochemical background map because the results of this method show the analysis of geochemical data in the frequency domain, which can provide new exploratory information that may not be revealed in the spatial domain, and since

the noise data is reduced from the results, the accuracy of determination of the thresholds can be higher than the other two applied methods.

References

- [1]. Zhao, P., Shundu, C. and Youngqing, C. (1996). A Thorough investigation of Geoanomaly: A basis of metallogenic prognosis. *Geological Journal of China Universities*. 2: 361-373.
- [2]. Zhao, P., (2007). Quantitative mineral prediction and deep mineral exploration. *Earth Science Frontiers*. 14 (5): 1.
- [3]. Liu, Y., Xia, Q., Cheng, Q. and Wang, X. (2013). Application of singularity theory and logistic regression model for tungsten polymetallic potential mapping. *Nonlinear Processes in Geophysics*. 20: 445-453.
- [4]. Bølviken, B., Stokke, P., Feder, J. and Jössang, T. (1992). The fractal nature of geochemical landscapes. *Journal of Geochemical Exploration*. 43: 91-109.
- [5]. Cheng, Q. and Agterberg, F.P. (1996). Multifractal modeling and spatial statistics. *Mathematical Geology*. 28: 1-16.
- [6]. Li, C., Ma, T. and Shi, J. (2003). Application of a fractal method relating concentrations and distances for separation of geochemical anomalies from background. *Journal of Geochemical Exploration*. 77: 167-175.
- [7]. Zhao, P. (1999). *Theory and Practice of Geoanomaly in Mineral Exploration*. China University of Geosciences Press. Wuhan. China. Chinese with English abstract. 150 P.
- [8]. Cheng, Q. (2007). Mapping singularities with stream sediment geochemical data for prediction of undiscovered mineral deposits in Gejiu, Yunnan Province, China. *Ore Geology Reviews*. 32: 314-324.
- [9]. Cheng, Q. and Agterberg, F.P. (2009). Singularity analysis of ore-mineral and toxic trace elements in stream sediments. *Computers & Geosciences*. 35: 234-244.
- [10]. Hawkes, H.E. and Webb, J.S. (1963). *Geochemistry in Mineral Exploration*. Soil Science. 95 (4): 283.
- [11]. Gałuszka, A. (2007). A review of geochemical background concepts and an example using data from Poland. *Environmental geology*. 52: 861-870.
- [12]. Cheng, Q., Agterberg, F. and Ballantyne, S. (1994). The separation of geochemical anomalies from background by fractal methods. *Journal of Geochemical Exploration*. 51: 109-130.
- [13]. Cheng, Q., Agterberg, F. and Bonham-Carter, G. (1996). A spatial analysis method for geochemical anomaly separation. *Journal of Geochemical Exploration*. 56: 183-195.
- [14]. Cheng, Q., Bonham-Carter, G., Hall, G. and Bajc, A. (1997). Statistical study of trace elements in the soluble organic and amorphous Fe-Mn phases of surficial sediments, Sudbury Basin. 1. Multivariate and spatial analysis. *Journal of Geochemical Exploration*. 59: 27-46.
- [15]. Cheng, Q. (1999). Multifractality and spatial statistics. *Computers & Geosciences*. 25: 949-961.
- [16]. Rafiee, A. (2005). Separating geochemical anomalies in stream sediment media by applying combination of fractal concentration-area model and multivariate analysis (Case study: Jeal-e-Barez 1: 100,000 Sheet, Iran), 20th World Mining Congress Proceeding, Iran. pp. 461-470.
- [17]. Salvadori, G., Ratti, S.P. and Belli, G. (1997). Fractal and multifractal approach to environmental pollution. *Environmental Science and Pollution Research*. 4: 91-98.
- [18]. Lima, A., De Vivo, B., Cicchella, D., Cortini, M. and Albanese, S. (2003). Multifractal IDW interpolation and fractal filtering method in environmental studies: an application on regional stream sediments of (Italy), Campania region. *Applied geochemistry*. 18: 1853-1865.
- [19]. Albanese, S., De Vivo, B., Lima, A. and Cicchella, D. (2007). Geochemical background and baseline values of toxic elements in stream sediments of Campania region (Italy). *Journal of Geochemical Exploration*. 93: 21-34.
- [20]. Cheng, Q. (1999). Spatial and scaling modelling for geochemical anomaly separation. *Journal of Geochemical Exploration*. 65: 175-194.
- [21]. Sinclair, A. (1991). A fundamental approach to threshold estimation in exploration geochemistry: probability plots revisited. *Journal of Geochemical Exploration*. 41: 1-22.
- [22]. Lin, Y.P. (2002). Multivariate geostatistical methods to identify and map spatial variations of soil heavy metals. *Environmental geology*. 42: 1-10.
- [23]. Mandelbrot, B.B. (1983). *The fractal geometry of nature*. Macmillan.
- [24]. Shen, W. and Cohen, D. (2005). Fractally invariant distributions and an application in geochemical exploration. *Mathematical Geology*. 37: 895-913.
- [25]. Deng, J., Wang, Q., Yang, L., Wang, Y., Gong, Q. and Liu, H. (2010). Delineation and explanation of geochemical anomalies using fractal models in the Heqing area, Yunnan Province, China. *Journal of Geochemical Exploration*. 105: 95-105.
- [26]. Sun, X., Gong, Q., Wang, Q., Yang, L., Wang, C. and Wang, Z. (2010). Application of local singularity model to delineate geochemical anomalies in Xiong'er shan gold and molybdenum ore district,

Western Henan province, China. *Journal of Geochemical Exploration*. 107: 21-29.

[27]. Lattuada, M., Wu, H. and Morbidelli, M. (2004). Radial density distribution of fractal clusters. *Chemical engineering science*. 59: 4401-4413.

[28]. Cheng, Q. (1995). The perimeter-area fractal model and its application to geology. *Mathematical Geology*. 27: 69-82.

[29]. Afzal, P., Alghalandis, Y.F., Khakzad, A., Moarefvand, P. and Omran, N.R. (2011). Delineation of mineralization zones in porphyry Cu deposits by fractal concentration-volume modeling. *Journal of Geochemical Exploration*. 108: 220-232.

[30]. Zuo, R. (2011). Decomposing of mixed pattern of arsenic using fractal model in Gangdese belt, Tibet, China. *Applied geochemistry*. 26: S271-S273.

[31]. Zuo, R. (2011). Identifying geochemical anomalies associated with Cu and Pb-Zn skarn mineralization using principal component analysis and spectrum-area fractal modeling in the Gangdese Belt, Tibet (China). *Journal of Geochemical Exploration*. 111: 13-22.

[32]. Gonçalves, M.A. (2001). Characterization of geochemical distributions using multifractal models. *Mathematical Geology*. 33: 41-61.

[33]. Ghannadpour, S.S. and Hezarkhani, A. (2015). Comparing U-statistic and nonstructural methods for separating anomaly and generating geochemical anomaly maps of Cu and Mo in Parkam district, Kerman, Iran. *Carbonates and Evaporites*. pp. 1-12.

[34]. Ghannadpour, S.S., Hezarkhani, A., Maghsoudi, A. and Farahbakhsh, E. (2015). Assessment of prospective areas for providing the geochemical anomaly maps of lead and zinc in Parkam district, Kerman, Iran. *Geosciences Journal*. 19: 431-440.

[35]. Pazand, K., Hezarkhani, A., Ataei, M. and Ghanbari, Y. (2011). Application of multifractal modeling technique in systematic geochemical stream sediment survey to identify copper anomalies: a case study from Ahar, Azarbaijan, Northwest Iran. *Chemie der Erde-Geochemistry*. 71: 397-402.

[36]. Mokhtari, Z., Boomeri, M. and Bagheri, S. (2015). Application of multifractal modeling technique in systematic litho-geochemical survey to identify Au-Cu anomalies in the Siah-Jangal area, Southeastern of Iran. *Arabian Journal of Geosciences*. 8: 9517-9530.

[37]. Meigoony, M.S., Afzal, P., Gholinejad, M., Yasrebi, A.B. and Sadeghi, B. (2014). Delineation of geochemical anomalies using factor analysis and multifractal modeling based on stream sediments data in Sarajeh 1: 100,000 sheet, Central Iran. *Arabian Journal of Geosciences*. 7: 5333-5343.

[38]. Nazarpour, A., Omran, N.R., Paydar, G.R., Sadeghi, B., Matroud, F. and Nejad, A.M. (2015).

Application of classical statistics, logratio transformation and multifractal approaches to delineate geochemical anomalies in the Zarshuran gold district, NW Iran. *Chemie der Erde-Geochemistry*. 75: 117-132.

[39]. Goncalves, M., Vairinho, M. and Oliveira, V. (1998). Study of geochemical anomalies in Mombeja area using a multifractal methodology and geostatistics. *IV IAMG*. 98: 590-595.

[40]. Sim, B., Agterberg, F.P. and Beaudry, C. (1999). Determining the cutoff between background and relative base metal smelter contamination levels using multifractal methods. *Computers & Geosciences*. 25: 1023-1041.

[41]. Wei, S. and Pengda, Z. (2002). Theoretical study of statistical fractal model with applications to mineral resource prediction. *Computers & Geosciences*. 28: 369-376.

[42]. Geranian, H., Mokhtari, A.R. and Cohen, D.R. (2013). A comparison of fractal methods and probability plots in identifying and mapping soil metal contamination near an active mining area, Iran. *Science of The Total Environment*. 463: 845-854.

[43]. Zuo, R., Xia, Q. and Zhang, D. (2013). A comparison study of the C-A and S-A models with singularity analysis to identify geochemical anomalies in covered areas. *Applied geochemistry*. 33: 165-172.

[44]. Cheng, Q. (2007). Multifractal imaging filtering and decomposition methods in space, Fourier frequency, and eigen domains. *Nonlinear Processes in Geophysics*. 14: 293-303.

[45]. Cheng, Q., Xu, Y. and Grunsky, E. (2000). Integrated spatial and spectrum method for geochemical anomaly separation. *Natural Resources Research*. 9: 43-52.

[46]. Xu, Y. and Cheng, Q. (2001). A multifractal filter technique for geochemical data analysis from Nova Scotia, Canada. *J Geochem Explor, Anal Environ*. 1: 1-12.

[47]. Panahi, A. and Cheng, Q. (2004). Multifractality as a measure of spatial distribution of geochemical patterns. *Mathematical Geology*. 36: 827-846.

[48]. Qiuming, C. (2006). Multifractal modelling and spectrum analysis: Methods and applications to gamma ray spectrometer data from southwestern Nova Scotia, Canada. *Science in China Series D*. 49: 283-294.

[49]. Ali, K., Cheng, Q. and Chen, Z. (2007). Multifractal power spectrum and singularity analysis for modelling stream sediment geochemical distribution patterns to identify anomalies related to gold mineralization in Yunnan Province, South China. *Geochemistry: Exploration, Environment, Analysis*. 7: 293-301.

- [50]. Afzal, P., Alghalandis, Y.F., Moarefvand, P., Omran, N.R. and Haroni, H.A. (2012). Application of power-spectrum–volume fractal method for detecting hypogene, supergene enrichment, leached and barren zones in Kahang Cu porphyry deposit, Central Iran. *Journal of Geochemical Exploration*. 112: 131-138.
- [51]. Afzal, P., Harati, H., Alghalandis, Y.F. and Yasrebi, A.B. (2013). Application of spectrum-area fractal model to identify of geochemical anomalies based on soil data in Kahang porphyry-type Cu deposit, Iran. *Chemie der Erde-Geochemistry*. 73: 533-543.
- [52]. Zuo, R. and Xia, Q. (2009). Application fractal and multifractal methods to mapping prospectivity for metamorphosed sedimentary iron deposits using stream sediment geochemical data in eastern Hebei province, China. *Geochimica et Cosmochimica Acta Supplement*. 73: A1540.
- [53]. Ge, Y., Cheng, Q. and Zhang, S. (2005). Reduction of edge effects in spatial information extraction from regional geochemical data: a case study based on multifractal filtering technique. *Computers & Geosciences*. 31: 545-554.
- [54]. Li, Q. and Cheng, Q. (2004). Fractal singular-value (eigen-value) decomposition method for geophysical and geochemical anomaly reconstruction. *Journal of China University of Geosciences*. 29: 109-118.
- [55]. Afzal, P., Ahmadi, K. and Rahbar, K. (2017). Application of fractal-wavelet analysis for separation of geochemical anomalies. *Journal of African Earth Sciences*. 128: 27-36.
- [56]. Woods, J., Biemond, J. and Tekalp, A. (1985). Boundary value problem in image restoration, *Acoustics, Speech, and Signal Processing, IEEE International Conference on ICASSP'85*. IEEE. pp. 692-695.
- [57]. Tekalp, A.M. and Sezan, M.I. (1990). Quantitative analysis of artifacts in linear space-invariant image restoration. *Multidimensional Systems and Signal Processing*. 1: 143-177.
- [58]. Aghdasi, F. and Ward, R.K. (1996). Reduction of boundary artifacts in image restoration. *IEEE Transactions on Image Processing*. 5: 611-618.
- [59]. Gonzalez, R.C. and Woods, R.E. (2002). *Digital image processing*. Prentice hall Upper Saddle River, NJ.

مطالعه مقایسه‌ای مدل‌های فرکتال و روش آماره U برای شناسایی آنومالی‌های ژئوشیمیایی؛ مطالعه موردی سیستم پورفیری آونج، ایران مرکزی

بشیر شکوه سلجوقی*، اردشیر هزارخانی و احسان فرح‌بخش

دانشکده مهندسی معدن و متالورژی، دانشگاه صنعتی امیرکبیر، ایران

ارسال ۲۰۱۷/۸/۱۳، پذیرش ۲۰۱۷/۹/۲۰

* نویسنده مسئول مکاتبات: b.shokouh@aut.ac.ir

چکیده:

مهم‌ترین جنبه برنامه اکتشاف ژئوشیمیایی، تعیین و جداسازی مقادیر آنومال از زمینه است. در دهه‌های گذشته، آنومالی‌های ژئوشیمیایی توسط روش‌های مختلفی شناسایی شده‌اند. اغلب روش‌های آماری معمول به کار برده شده در تعیین آستانه‌های غلظت ژئوشیمیایی برای جداسازی آنومالی‌های از زمینه، کارایی محدودی در نواحی با محیط‌های زمین‌شناسی پیچیده دارند. در این مطالعه، سه روش، شامل مدل‌های فرکتال غلظت-مساحت (C-A)، طیف-مساحت (S-A) و آماره U برای شناسایی آنومالی‌های ژئوشیمیایی در سیستم پورفیری آونج با توجه به محیط زمین‌شناسی و تکتونیک پیچیده ناحیه به کار برده شده است. نتایج به دست آمده نشان داد که روش‌های S-A و آماره U نتایج قابل قبول‌تری را نسبت به روش C-A نشان می‌دهند. مدل C-A در شناسایی آنومالی‌های ژئوشیمیایی درون ناحیه‌ای شامل زمینه ژئوشیمیایی ساده خوب عمل می‌کند که هر زیر ناحیه توسط میدان ژئوشیمیایی مشخص شده است. روش آماره U با در نظر گرفتن مکان نقاط نمونه‌برداری، ارتباط فضایی آن‌ها و شعاع تأثیر برای هر نقطه در تخمین مکان آنومالی، بر محدودیت‌های مدل C-A غلبه می‌کند. مدل S-A ابزاری قدرتمند برای تجزیه الگوهای ژئوشیمیایی پیچیده به نقشه آنومالی ژئوشیمیایی و نقشه زمینه ژئوشیمیایی است. خروجی این روش، تجزیه و تحلیل داده‌های ژئوشیمیایی را در حوزه فرکانس نشان می‌دهد که می‌تواند اطلاعات اکتشافی جدیدی را فراهم آورد که ممکن نیست در حوزه فضایی آشکار شوند. نهایتاً، می‌توان اشاره کرد که صحت مدل فرکتال S-A برای تعیین آستانه‌ها بالاتر از دو روش ذکر شده دیگر است.

کلمات کلیدی: فرکتال C-A، مولتی‌فرکتال S-A، آنومالی ژئوشیمیایی، جدایش آنومالی، آماره U، سیستم پورفیری آونج.